

# Ising Meson Spectroscopy on a Noisy Digital Quantum Simulator

Christopher Lamb,<sup>\*</sup> Yicheng Tang, Robert Davis, and Ananda Roy<sup>†</sup>

*Department of Physics and Astronomy, Rutgers University, Piscataway, NJ 08854-8019 USA*

Quantum simulation has the potential to be an indispensable technique for the investigation of non-perturbative phenomena in strongly-interacting quantum field theories (QFTs). In the modern quantum era, with Noisy Intermediate Scale Quantum (NISQ) simulators widely available and larger-scale quantum machines on the horizon, it is natural to ask: what non-perturbative QFT problems can be solved with the existing quantum hardware? We show that existing noisy quantum machines can be used to analyze the energy spectrum of a large family of strongly-interacting 1+1D QFTs. The latter exhibit a wide-range of non-perturbative effects like ‘quark confinement’ and ‘false vacuum decay’ which are typically associated with higher-dimensional QFTs of elementary particles. We perform quench experiments on IBM’s `ibm_auckland` and `ibmq_mumbai` quantum simulators to compute the energy spectrum of 1+1D quantum Ising model with a longitudinal field. The latter model is particularly interesting due to the formation of mesonic bound states arising from a confining potential for the Ising domain-walls, reminiscent of t’Hooft’s model of two-dimensional quantum chromodynamics. Our results demonstrate that digital quantum simulation in the NISQ era has the potential to be a viable alternative to numerical techniques such as density matrix renormalization group or the truncated conformal space methods for analyzing QFTs.

Investigation of non-perturbative phenomena in strongly interacting quantum field theories (QFTs) remains one of the outstanding challenges of modern physics. Despite impressive progress, ab-initio lattice computations of properties of arbitrary QFTs will likely remain beyond the computational capabilities of the most powerful classical computer. This is due to the exponentially-growing Hilbert space which poses an insurmountable challenge for exact simulation of these lattice models. Nevertheless, quasi-exact or approximate classical computing techniques have been successful in investigating a large family of quantum many-body systems that realize QFTs in the scaling limit. For example, states with ‘relatively low entanglement’ can be efficiently represented using tensor networks [1–4]. This has allowed high-precision investigation of low-energy states of one-dimensional, local, gapped and gapless Hamiltonians using matrix product states [5] as well as their two-dimensional generalizations [6, 7].

Despite the success of classical computing methods, simulation of high-energy states or non-equilibrium dynamics remains challenging even for generic, strongly-interacting 1+1D quantum systems. This is due to the rapid growth of entanglement between different subsystems [8–11]. Quantum simulation, both analog and digital, have the potential to become a viable alternative to the aforementioned approaches for tackling these questions [12, 13]. Analog quantum simulation involves tailoring a given quantum system to emulate a specific target model [14–19] and has been remarkably successful in analyzing a wide range of physical problems. However, it is gate-based, error-corrected, digital quantum simulation that is the long-term, universal solution for simulation of QFTs [20]. In this approach, lattice regularizations of QFTs can be encoded into registers of error-corrected qubits with suitable initial state preparation, time evolution and measurement protocols.

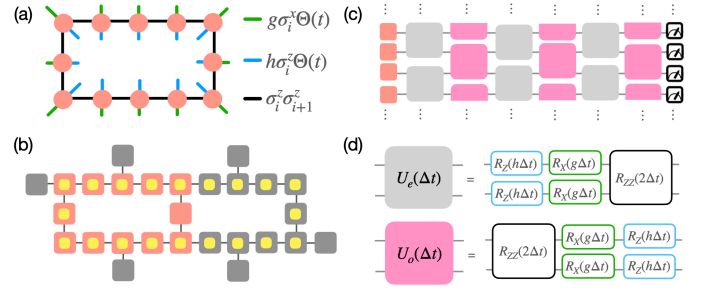


FIG. 1. (a) Schematic of the periodic Ising chain. The coral circles indicate spin-1/2 sites. The black, green and blue bonds respectively correspond to the ferromagnetic interaction, transverse and longitudinal fields respectively. The quench protocol involves turning on, at  $t = 0$ , the longitudinal and transverse field strengths:  $g \leq 1, h < 1$  in the Hamiltonian  $H$  [Eq. (1)]. The system is initially prepared in the ground state of  $H$  with  $g = h = 0$ :  $|\uparrow, \dots, \uparrow\rangle$ . (b) Schematic of the qubit layout in IBM’s `ibm_auckland` and `ibmq_mumbai` quantum simulators. Of the available 27 qubits (in gray), a periodic chain of 12 qubits (in coral) and 20 qubits (in yellow) were chosen for the quench experiments. (c) Schematic of the trotterized unitary time-evolution generated by  $H$ . The action of the full unitary operator is decomposed into the unitary operators:  $U_e$  and  $U_o$ . At the end of the time-evolution, single qubit measurements are performed in the  $\sigma_y$  basis. (d) The decompositions of  $U_e$  and  $U_o$  in terms of single and two qubit gates are shown.

However, implementing such a quantum simulation protocol on existing quantum hardware remains a daunting challenge. In spite of the recent progress in the fab-

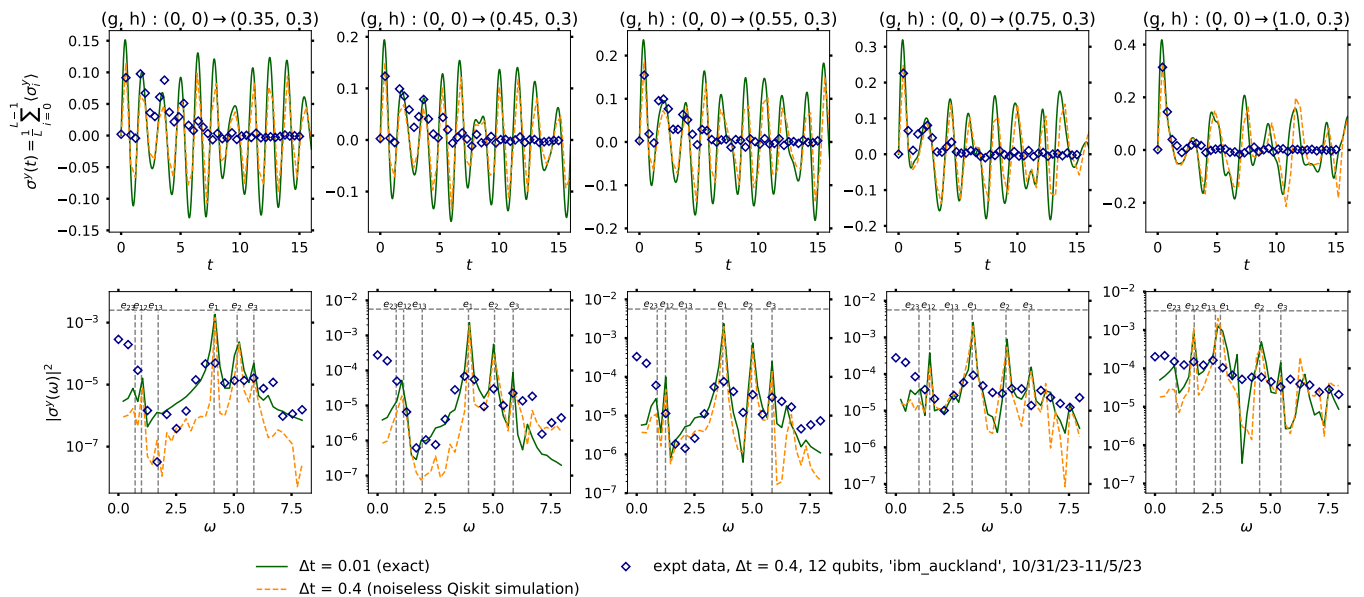


FIG. 2. Ising meson spectroscopy simulation and experimental results for quench from  $g = h = 0$  using pulse-efficient quantum circuits (see Supplementary Note I). The Qiskit twirled readout error extinction and dynamical decoupling schemes were used to mitigate the effects of noise present in the `ibm_auckland` simulator. (Top panels) Results for  $\sigma^y(t) = \sum_j \langle \sigma_j^y(t) \rangle / L$  for different quench parameters are shown. A periodic chain with length  $L = 12$  qubits (in coral in Fig. 1) was used for quenches to  $g \leq 1$  with  $h = 0.3$ . The results obtained using exact simulation of the time evolution of  $L$  qubits with  $\Delta t = 0.01$  are shown with green solid lines. The noiseless numerical Qiskit simulation results are performed for  $\Delta t = 0.4$  (orange dashed line). The expectation values for the noiseless simulations are computed by trotterized time-evolution and making measurements in the  $\sigma^y$  basis for each qubit after every time-step and averaging over 5 runs with 8192 shots each. The experimental data from the quantum hardware are shown as blue diamonds. (Bottom panels) The squared absolute values of the Fourier transforms  $\sigma^y(\omega)$  are shown. The peaks in the latter correspond to the rest energies ( $e_n$ ), of the mesonic excitations labeled by  $n$ , and their differences ( $e_{mn}$ ). The gray dashed lines correspond to the exact diagonalization results obtained in the zero momentum sector. As shown in the bottom panels, the lowest meson energy is clearly discernible except for the rightmost panel, where the close proximity of the numerical values of  $e_1$  and  $e_{13}$  prevent an unambiguous identification.

rication and manipulation photonic and solid-state systems, the number of available qubits across the different quantum computing platforms remains around  $10^2$  with modest coherence times. Given the large overhead in the number of required qubits to implement quantum error correcting codes [25], it is an open problem to implement error-corrected digital simulation of QFTs in the near term. This raises the question: *what non-perturbative QFT problems can be tackled with current Noisy Intermediate Scale Quantum (NISQ) machines?*

In this work, a superconducting NISQ simulator is used to compute the energy spectra of certain strongly-interacting QFTs that arise as scaling limits of one-dimensional quantum spin chains. The latter QFTs offer a valuable playground for investigation of a wide range of non-perturbative phenomena such as ‘quark confinement’ [26] and ‘false vacuum decay’ [27] that are typically associated with QFTs in higher-dimensions. Importantly, there are two practical advantages: i) these spin-chains can be directly mapped to arrays of qubits without additional overhead involved in discretizing the local lattice degree of freedom, ii) several properties of

these spin-chains can be investigated with existing classical numerical techniques (tensor networks) and analytical methods (Bethe ansatz and bosonization). This enables benchmarking NISQ simulators before using them for investigation of problems that truly lie beyond the reach of the classical computers.

The goal of this work is to demonstrate the aforementioned using the paradigmatic example of the one-dimensional quantum Ising model in the presence of a longitudinal field [28]. The Hamiltonian is

$$H = - \sum_{j=1}^L (\sigma_j^z \sigma_{j+1}^z + g \sigma_j^x + h \sigma_j^z), \quad (1)$$

where  $g, h$  are the strengths of the transverse and longitudinal fields and we have chosen periodic boundary conditions. We consider the case  $g \leq 1, h < 1$ . The presence of the longitudinal field introduces a confining potential between the domain-wall excitations of the Ising model. This leads to formation of ‘mesonic’ bound states, analogous to hadron-formation in quantum chromodynamics [29, 30]. The energy spectrum has been analyzed using semi-classical [31, 32], truncated conformal

space [33–37] and exact diagonalization [38] approaches. While signatures of confinement have been observed for this model in a NISQ simulator [39] (see also Ref. [40] for analysis of a related model), digital quantum simulation of the energy spectrum has remained elusive. This is performed in this work using a quench experiment on IBM’s `ibm_auckland` simulator which is one of the IBM Quantum Falcon Processors. The quantum simulation protocol is first tested using the Qiskit software package [41] and benchmarked against exact computations. Subsequently, it is implemented on the noisy quantum hardware.

The quantum simulation protocol is as follows (see Fig. 1). First, the qubits are prepared in the state:  $|\uparrow, \dots, \uparrow\rangle$ , which is one of the two degenerate ground state of the Hamiltonian  $H$  with  $g = h = 0$  [42]. Next, a global quench is performed to  $0 < g \leq 1, h < 1$  on the 12 qubit loop (in coral in Fig. 1) of the `ibm_auckland` simulator. The quench is implemented in the NISQ hardware by the application of single and two-qubit gates [Fig. 1(c,d)] [43] that together give rise to the unitary operator  $U = e^{-iH\Delta t}$ . Here,  $\Delta t$  is the size of the time-step. The rest energy spectrum of the mesonic excitations formed due to the confinement of fermionic Ising domain-walls manifests itself in the observables that involve only single-qubit operators [38]. This is particularly suitable for implementation in a NISQ machine where single qubit measurements are performed with relatively low error. In particular, in this work, the single-qubit observable  $\langle \sigma_j^y(t) \rangle$ ,  $j$  being the site-index, is measured during the course of this evolution [44].

Fig. 2 shows the results for the quenches from  $g = h = 0$  to  $g \leq 1, h = 0.3$ . The top panels show the measured variation of  $\sigma^y(t) = \sum_j \langle \sigma_j^y(t) \rangle / L$  with time. The solid green curves act as reference and are obtained from exact computation of the time-evolution of the chain of qubits with  $\Delta t = 0.01$  [45]. The dashed orange curves are obtained from numerical simulations on a noiseless Qiskit simulator for  $\Delta t = 0.4$ . In this case, the expectation value  $\langle \sigma_j^y(t) \rangle$  was computed for each qubit at each time-step by measuring it in the corresponding basis and averaging over 8192 shots. The close agreement of the noiseless simulation results for the two choices of  $\Delta t$  indicates a small trotterization error for this observable. The quantum simulation experiment on `ibm_auckland` was performed with the same parameters as the noiseless simulations (experimental data as blue diamonds in Fig. 2). To mitigate the effects of qubit and gate errors on the quantum hardware, a pulse-efficient quantum circuit was implemented (see Supplementary Note I) in addition to the in-built Qiskit twirled readout error extinction and dynamical decoupling schemes. The bottom panels show the absolute values of the corresponding Fourier transforms. The rest energies of the mesons are inferred from the location of the peaks, with the dashed vertical lines being results obtained using exact diagonalization

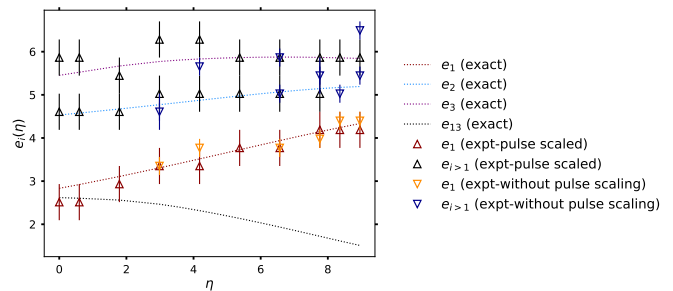


FIG. 3. Variation of the meson energies obtained from quantum simulation experiments performed on the `ibm_auckland` (with pulse-scaling) and `ibmq_mumbai` (without pulse-scaling) simulators. The results (triangles) are shown for a quench from  $g = h = 0$  to  $g \in [0.25, 1.0]$  and  $h = 0.3$ . The corresponding predictions from exact diagonalization of the 12-site qubit chain keeping only the translation-invariant states are shown as dotted lines. The meson energies are shown as a function of the dimensionless parameter  $\eta = 2\pi(1 - g)/h^{8/15}$ . The peaks for the different meson energies were identified by computing the  $\sigma^y(\omega)$  for quenching to different choices of  $g$  (Fig. 2). Note that the obtained quantum data did not always permit unambiguous identification of the second and third meson energies. Furthermore, for the smallest three values of  $\eta$ , the difference between the first and the third meson energies (black dotted line) is also close to the obtained peak in the spectral function (see also rightmost panels of Fig. 2). Smaller trotterization steps would enable identification of the lowest meson energies for these choice of parameters, but additional error-mitigation techniques will be necessary.

in the zero momentum sector. Note that the quality of the data from the quantum hardware for  $g = 1$  is worse than the  $g < 1$  cases. This is due to the lower gap between the ground and first excited states of the energy spectrum. This makes the experiments more susceptible to the noise arising due to trotterization and noise in the `ibm_auckland` simulator. In addition, for the  $g = 1$  case, the numerical values of  $e_{13}$  and  $e_1$  are close to each other (see dashed lines in bottom right panel of Fig. 2). This prevents an unambiguous identification of the lowest meson energy in this particular case already with the exact computation performed using  $\Delta t = 0.01$  (solid green lines). We note that even though the obtained amplitude of the time-series data decays rapidly due to decoherence and gate errors, the frequency, which contains the information of the meson energies, is still discernible. This is true also for other analyzed models, see Supplementary Note II.

Fig. 3 shows the variation of the meson energies obtained from different quench experiments performed on the `ibm_auckland` simulator. In every experiment, the system was initialized in the ground state of  $g = h = 0$ . Subsequently, a quench was performed to  $h = 0.3$  and  $g$  varying between 0.25 and 1.0. The obtained meson energies are shown as diamonds. The corresponding pre-

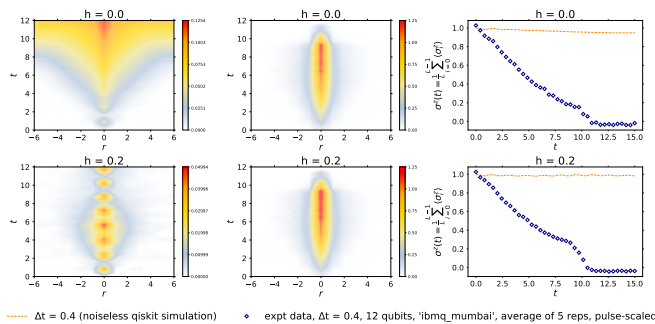


FIG. 4. Results for  $G_z(r, t)$  and the  $\langle \sigma^z(t) \rangle$  for a quench to  $g = 0.25, h = 0$  and  $g = 0.25, h = 0.2$ . The noiseless simulation results for  $G_z(r, t)$  are shown in the left panels. The corresponding results for  $\sigma^z(t)$  are shown with orange dashed lines in the right panels. The simulation parameters are the same as in Fig. 2. The results of the quantum simulation experiments on the `ibmq_mumbai` simulator are shown in the middle panel and with blue diamonds in the right panel. With the current noisy gates and qubits on the quantum hardware, a distinct signature of confinement could not be discerned. This is consistent with the rapid decay of  $\langle \sigma^z(t) \rangle$  (blue diamonds in the right panels). Additional error mitigation techniques and improved quantum hardware can be used to obtain more reliable signatures of the confinement in the correlation functions.

dictions from the exact diagonalization of the qubit chain in the zero momentum sector are shown as dotted lines. Notice that the noisy data did not always permit unique identification of the second and third meson energies. Furthermore, for the three smallest values of  $\eta$ , the lowest meson energy ( $e_1$ ) is close in numerical value to the difference between the first and third meson energies ( $e_{13}$ ). To uniquely identify between  $e_1$  and  $e_{13}$  for these three values of parameters, smaller trotterization steps and additional error mitigation techniques will be necessary.

Fig. 4 shows the results for the connected correlation function  $G_z(r, t) = \langle \sigma_i^z(t) \sigma_{i+r}^z(t) \rangle - \langle \sigma_i^z(t) \rangle \langle \sigma_{i+r}^z(t) \rangle$ . The latter contains signatures of the confinement of the domain-walls into mesonic excitations [38]. The results of the noiseless Qiskit simulations are shown in the left panels. The simulation parameters are kept as in Fig. 2. For  $h = 0$ , the correlation function exhibits a characteristic broadening due to the propagation of the energy-carrying domain wall excitations [8] until the separation between the latter is of the order of the system size (top left panel). For  $h \neq 0$ , as the domain-walls get separated, they feel the confining force that leads to the formation of the mesonic bound states. This results in oscillatory behavior of the correlation function [38] (bottom left panel). The corresponding expectation value  $\sigma^z(t) = \sum_j \langle \sigma_j^z(t) \rangle / L$  for the noiseless simulations are shown with the dashed orange line in the right panels. The data from the quantum hardware is shown in the middle panels. With the current noise levels in the gates and modest lifetimes of the qubits of the `ibmq_mumbai` simulator, signatures of

confinement could not be reliably discerned for the noisy experimental data for the correlation function. This is consistent with the measured rapid decay of  $\sigma^z(t)$  shown with blue diamonds in the right panel (compare the oscillations obtained for  $\langle \sigma^y(t) \rangle$  shown in Fig. 2). Additional error mitigation techniques and improved quantum hardware could be used to obtain signatures of confinement in the correlation functions.

In summary, this work highlights the potential of NISQ simulators for investigation of non-perturbative problems in strongly-interacting QFTs. In particular, a noisy IBM simulator is used to compute the energy-spectrum of the mesonic excitations occurring in the one-dimensional Ising model with a longitudinal field. The demonstrated quantum simulation scheme can be straightforwardly generalized to analyze a wide family of 1+1D QFTs. A natural extension is the quantum sine-Gordon model perturbed by a cosine potential with twice the periodicity. This model can be realized as the scaling limit of the XYZ spin chain [46] in the presence of a longitudinal field. In the latter model, the free Ising domain walls are replaced by interacting sine-Gordon solitons [47–50]. For details of the simulation protocol and corresponding results, see Supplementary Note II. With improved noise mitigation techniques that are likely to be available in the coming years, it is conceivable that a wider range of QFTs will become amenable to quantum simulation on quantum hardware. This can lead to investigation of a wide range of exotic QFT phenomena ranging from false-vacuum decays [51, 52] to Bloch oscillations [53, 54] in table-top quantum simulation experiments.

The authors acknowledge discussions with Nicholas Bronn, Robert Konik and Olivia Lanes and the use of IBM Quantum services for this work. The views expressed are those of the authors, and do not reflect the official policy or position of IBM or the IBM Quantum team. This work was supported by the U.S. Department of Energy, Office of Basic Energy Sciences, under Contract No. DE-SC0012704.

\* [cdl92@physics.rutgers.edu](mailto:cdl92@physics.rutgers.edu)

† [ananda.roy@physics.rutgers.edu](mailto:ananda.roy@physics.rutgers.edu)

- [1] M. B. Hastings, An area law for one-dimensional quantum systems, *J. Stat. Mech.* **0708**, P08024 (2007), [arXiv:0705.2024](https://arxiv.org/abs/0705.2024) [quant-ph].
- [2] G. Vidal, Class of quantum many-body states that can be efficiently simulated, *Phys. Rev. Lett.* **101**, 110501 (2008).
- [3] N. Schuch, M. M. Wolf, F. Verstraete, and J. I. Cirac, Entropy scaling and simulability by matrix product states, *Phys. Rev. Letters* **100**, 10.1103/physrevlett.100.030504 (2008).
- [4] F. Verstraete, V. Murg, and J. Cirac, Matrix product states, projected entangled pair states, and variational

- renormalization group methods for quantum spin systems, *Advances in Physics* **57**, 143 (2008).
- [5] U. Schollwöck, The density-matrix renormalization group in the age of matrix product states, *Annals of Physics* **326**, 96 (2011), january 2011 Special Issue.
- [6] N. Schuch, M. M. Wolf, F. Verstraete, and J. I. Cirac, Computational complexity of projected entangled pair states, *Phys. Rev. Lett.* **98**, 140506 (2007).
- [7] M. P. Zaletel and F. Pollmann, Isometric tensor network states in two dimensions, *Phys. Rev. Lett.* **124**, 037201 (2020).
- [8] P. Calabrese and J. Cardy, Evolution of entanglement entropy in one-dimensional systems, *Journal of Statistical Mechanics: Theory and Experiment* **2005**, P04010 (2005).
- [9] G. Vidal, Classical simulation of infinite-size quantum lattice systems in one spatial dimension, *Phys. Rev. Lett.* **98**, 070201 (2007).
- [10] S. Paeckel, T. Köhler, A. Swoboda, S. R. Manmana, U. Schollwöck, and C. Hubig, Time-evolution methods for matrix-product states, *Annals of Physics* **411**, 167998 (2019).
- [11] S.-H. Lin, M. P. Zaletel, and F. Pollmann, Efficient simulation of dynamics in two-dimensional quantum spin systems with isometric tensor networks, *Phys. Rev. B* **106**, 10.1103/physrevb.106.245102 (2022).
- [12] R. P. Feynman, Simulating Physics with Quantum Computers, *International Journal of Theoretical Physics* **21**, 467 (1982).
- [13] S. Lloyd, Universal Quantum Simulators, *Science* **273**, 1073 (1996).
- [14] B. Douçot, L. B. Ioffe, and J. Vidal, Discrete non-abelian gauge theories in josephson-junction arrays and quantum computation, *Phys. Rev. B* **69**, 214501 (2004).
- [15] J. I. Cirac, P. Maraner, and J. K. Pachos, Cold atom simulation of interacting relativistic quantum field theories, *Phys. Rev. Lett.* **105**, 190403 (2010).
- [16] H. P. Büchler, M. Hermele, S. D. Huber, M. P. A. Fisher, and P. Zoller, Atomic quantum simulator for lattice gauge theories and ring exchange models, *Phys. Rev. Lett.* **95**, 040402 (2005).
- [17] J. Casanova, L. Lamata, I. L. Egusquiza, R. Gerritsma, C. F. Roos, J. J. García-Ripoll, and E. Solano, Quantum simulation of quantum field theories in trapped ions, *Phys. Rev. Lett.* **107**, 260501 (2011).
- [18] C. Gross and I. Bloch, Quantum simulations with ultracold atoms in optical lattices, *Science* **357**, 995 (2017), <https://science.sciencemag.org/content/357/6355/995.full.pdf>.
- [19] A. Roy and H. Saleur, Quantum electronic circuit simulation of generalized sine-gordon models, *Phys. Rev. B* **100**, 155425 (2019).
- [20] S. P. Jordan, K. S. M. Lee, and J. Preskill, Quantum Algorithms for Quantum Field Theories, *Science* **336**, 1130 (2012), [arXiv:1111.3633 \[quant-ph\]](https://arxiv.org/abs/1111.3633).
- [21] A. Macridin, P. Spentzouris, J. Amundson, and R. Harnik, Digital quantum computation of fermion-boson interacting systems, *Phys. Rev. A* **98**, 10.1103/physreva.98.042312 (2018).
- [22] N. Klco and M. J. Savage, Digitization of scalar fields for quantum computing, *Phys. Rev. A* **99**, 10.1103/physreva.99.052335 (2019).
- [23] S. P. Jordan, K. S. M. Lee, and J. Preskill, Quantum Computation of Scattering in Scalar Quantum Field Theories, *Quant. Inf. Comput.* **14** (2014), [arXiv:1112.4833 \[hep-th\]](https://arxiv.org/abs/1112.4833).
- [24] S. P. Jordan, K. S. M. Lee, and J. Preskill, Quantum Algorithms for Fermionic Quantum Field Theories, (2014), [arXiv:1404.7115 \[hep-th\]](https://arxiv.org/abs/1404.7115).
- [25] M. A. Nielsen and I. L. Chuang, *Quantum Computation and Quantum Information* (Cambridge University Press, 2000).
- [26] J. Greensite, *An introduction to the confinement problem*, Vol. 821 (2011).
- [27] S. Coleman, *Aspects of Symmetry: Selected Erice Lectures* (Cambridge University Press, 1988).
- [28] B. M. McCoy and T. T. Wu, Two-dimensional ising field theory in a magnetic field: Breakup of the cut in the two-point function, *Phys. Rev. D* **18**, 1259 (1978).
- [29] G. 't Hooft, A two-dimensional model for mesons, *Nuclear Physics B* **75**, 461 (1974).
- [30] A. Zamolodchikov, Integrable field theory from conformal field theory, in *Integrable Sys Quantum Field Theory*, edited by M. Jimbo, T. Miwa, and A. Tsuchiya (Academic Press, San Diego, 1989) pp. 641 – 674.
- [31] S. B. Rutkevich, Large- $n$  excitations in the ferromagnetic ising field theory in a weak magnetic field: Mass spectrum and decay widths, *Phys. Rev. Lett.* **95**, 250601 (2005).
- [32] S. B. Rutkevich, Energy spectrum of bound-spinons in the quantum ising spin-chain ferromagnet, *J. Stat. Phys.* **131**, 917 (2008).
- [33] P. Fonseca and A. Zamolodchikov, Ising field theory in a magnetic field: Analytic properties of the free energy, *J. Stat. Phys.* **110**, 527 (2003).
- [34] P. Fonseca and A. Zamolodchikov, Ising spectroscopy. I. Mesons at  $T < T_c$ , (2006), [arXiv:hep-th/0612304](https://arxiv.org/abs/hep-th/0612304).
- [35] A. J. A. James, R. M. Konik, and N. J. Robinson, Non-thermal states arising from confinement in one and two dimensions, *Phys. Rev. Lett.* **122**, 130603 (2019).
- [36] N. J. Robinson, A. J. A. James, and R. M. Konik, Signatures of rare states and thermalization in a theory with confinement, *Phys. Rev. B* **99**, 195108 (2019).
- [37] T. Rakovszky, M. Mestyán, M. Collura, M. Kormos, and G. Takács, Hamiltonian truncation approach to quenches in the Ising field theory, *Nucl. Phys. B* **911**, 805 (2016), [arXiv:1607.01068 \[cond-mat.stat-mech\]](https://arxiv.org/abs/1607.01068).
- [38] M. Kormos, M. Collura, G. Takács, and P. Calabrese, Real-time confinement following a quantum quench to a non-integrable model, *Nature Physics* **13**, 246 (2016).
- [39] J. Vovrosh and J. Knolle, Confinement and entanglement dynamics on a digital quantum computer, *Scientific Reports* **11**, 11577 (2021).
- [40] W. L. Tan, P. Becker, F. Liu, G. Pagano, K. S. Collins, A. De, L. Feng, H. B. Kaplan, A. Kyprianidis, R. Lundgren, W. Morong, S. Whitsitt, A. V. Gorshkov, and C. Monroe, Domain-wall confinement and dynamics in a quantum simulator, *Nature Physics* **17**, 742 (2021).
- [41] A. tA-v et al, *Qiskit: An open-source framework for quantum computing* (2021).
- [42] The protocol could be implemented also with the initial state being the ground state of the Hamiltonian with  $g < 1, h = 0$ . However, preparing such an initial state on a quantum simulator is nontrivial [55–57]. For simplicity, we restrict ourselves to initial product states.
- [43] A. Smith, M. S. Kim, F. Pollmann, and J. Knolle, Simulating quantum many-body dynamics on a current digital quantum computer, *npj Quantum Inf.* **5**, 106 (2019), [arXiv:1906.06343 \[quant-ph\]](https://arxiv.org/abs/1906.06343).

- [44] The meson rest energy spectrum can be also computed by measuring  $\langle \sigma_j^x(t) \rangle$  or  $\langle \sigma_j^z(t) \rangle$ . On a noisy simulator, the best noise-resilience for the energy computation was obtained for  $\langle \sigma_j^y(t) \rangle$ . The same choice was found to be optimal with regards to the errors arising from trotterization of the continuous time-evolution.
- [45] Exact simulation of  $g = 1$  with 20 qubits was challenging for the classical computational resources available for this work. This case was computed with Qutip [58, 59].
- [46] R. Baxter, *Exactly Solved Models in Statistical Mechanics*, Dover Books on Physics (Dover Publications, 2013).
- [47] G. Delfino and G. Mussardo, Non-integrable aspects of the multi-frequency sine-gordon model, *Nuclear Physics B* **516**, 675–703 (1998).
- [48] Z. Bajnok, L. Palla, G. Takacs, and F. Wagner, Nonperturbative study of the two frequency sine-Gordon model, *Nucl. Phys. B* **601**, 503 (2001), [arXiv:hep-th/0008066](https://arxiv.org/abs/hep-th/0008066).
- [49] G. Mussardo, V. Riva, and G. Sotkov, Semiclassical particle spectrum of double sine-Gordon model, *Nucl. Phys. B* **687**, 189 (2004), [arXiv:hep-th/0402179](https://arxiv.org/abs/hep-th/0402179).
- [50] A. Roy and S. L. Lukyanov, Soliton confinement in a quantum circuit, *Nature Commun.* **14**, 7433 (2023), [arXiv:2302.06289](https://arxiv.org/abs/2302.06289) [quant-ph].
- [51] G. Lagnese, F. M. Surace, M. Kormos, and P. Calabrese, False vacuum decay in quantum spin chains, *Phys. Rev. B* **104**, L201106 (2021).
- [52] M. Lencsés, G. Mussardo, and G. Takács, Variations on vacuum decay: The scaling ising and tricritical ising field theories, *Phys. Rev. D* **106**, 105003 (2022).
- [53] A. Lerose, F. M. Surace, P. P. Mazza, G. Peretto, M. Collura, and A. Gambassi, Quasilocalized dynamics from confinement of quantum excitations, *Phys. Rev. B* **102**, 041118 (2020).
- [54] O. Pomponio, M. A. Werner, G. Zarand, and G. Takacs, Bloch oscillations and the lack of the decay of the false vacuum in a one-dimensional quantum spin chain, *SciPost Phys.* **12**, 061 (2022).
- [55] F. Verstraete, J. I. Cirac, and J. I. Latorre, Quantum circuits for strongly correlated quantum systems, *Phys. Rev. A* **79**, 032316 (2009).
- [56] W. W. Ho and T. H. Hsieh, Efficient variational simulation of non-trivial quantum states, *SciPost Phys.* **6**, 029 (2019).
- [57] A. Roy, S. Erramilli, and R. M. Konik, Efficient Quantum Circuits based on the Quantum Natural Gradient, *arXiv e-prints*, [arXiv:2310.10538](https://arxiv.org/abs/2310.10538) (2023), [arXiv:2310.10538](https://arxiv.org/abs/2310.10538) [quant-ph].
- [58] J. Johansson, P. Nation, and F. Nori, Qutip: An open-source python framework for the dynamics of open quantum systems, *Computer Physics Communications* **183**, 1760 (2012).
- [59] J. Johansson, P. Nation, and F. Nori, Qutip 2: A python framework for the dynamics of open quantum systems, *Computer Physics Communications* **184**, 1234 (2013).